THE PROBLEM OF HEADING ESTIMATION IN SYNTHETIC APERTURE SONAR

G.A.Shippey[+], M. Jonsson[#], E.Parastates[#] and J. Pihl[#]
+Queensferry Consultants Ltd.,31 Palmerston Place, Edinburgh, Scotland
FOI, Swedish Defence Research Agency, SE-172 90 Stockholm, Sweden
mattiasj@foi.se

Abstract

Synthetic Aperture Sonar (SAS) is extremely dependent on correct positioning. Various techniques have been developed, such as the Displaced Phase-Centre Array (DPCA) method. Here correlations between seabed echoes arriving at the DPCA's are used to estimate both sway (lateral movement of the platform) and change of heading between pings. However it is difficult to estimate heading change with the required accuracy by DPCA methods. Small calibration errors, or deviations in the seabed model from an isotropic reflector distribution, accumulate to significant heading errors over many pings. Moreover, for a specific target object, range and look angle to the target are more useful parameters than sway and heading. DPCA autopositioning on target echoes gives the parameters required. Furthermore, sufficiently accurate look-angle estimates can be made using the centroid of the physical aperture target image, generated from each track position. Experimental results are presented showing successful SAS imaging, with no *a priori* knowledge of heading, track, or platform speed over the seabed.

1. Introduction

There are many references, eg [1,2] to displaced phase-centre array (DPCA) autopositioning (autofocus, micronavigation), using seabed echoes from a sidescan swath abeam of the sonar platform. Leading and trailing subarrays of equal length are chosen from the whole receiver array. Echoes received by the leading subarray are correlated with echoes of the following ping received by the trailing subarray. If separation between subarray centres is approximately twice platform movement between pings, then the phase-centre subarrays remain approximately stationary between pings. It is then possible to correlate echoes from random reflector distributions, giving the down-range displacement of each phase-centre channel from one ping to the next.

Ping-to-ping corrections can be summed along the aperture in order to correct sway and heading errors in the basic navigation system. However sway and heading are secondary for imaging a specific target. The primary parameters are radial distance from the target and look-angle. Section 2 shows that these parameters are obtained more directly by DPCA correlation of target echoes. For compact targets, it can be preferable to determine look-angle directly from the principal direction of echo arrival (DOA). This can be determined using the centroid of the physical aperture image generated at each platform position. The accuracy of this method will be shown by simulation and with experimental data.

2. Autopositioning with respect to Compact Target

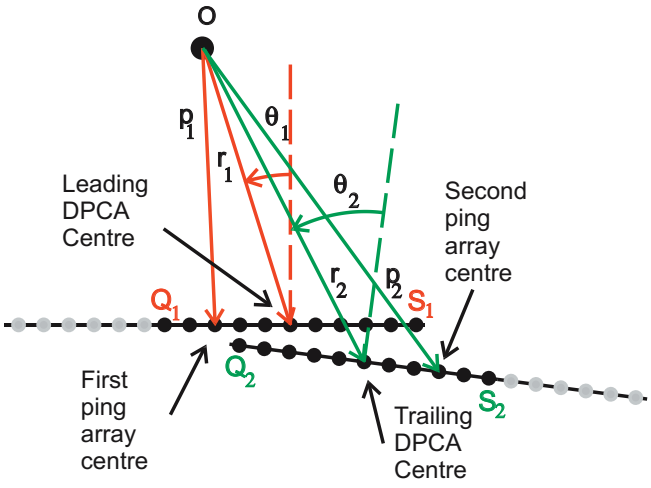

Fig 2.1. DPCA Geometry for Compact Target

2.1 Theory

In Fig 2.1 is Q_1S_1 the leading ping sub-array and Q_2S_2 the trailing ping sub-array, of lengths D. p1 and p2 are the ranges between a point reflector O and the array centre at the two pings. r_1 and r_2 are the ranges between the two DPCA centres and O. θ_1, θ_2 are look-angles to O wrt each array normal. Then if D<< r and the range OQ_1 are denoted q1 etc.

$q_1 = r_1 - \frac{1}{2}D \sin\theta_1$
$s_1 = r_1 + \frac{1}{2}D \sin\theta_1$
$q_2 = r_2 - \frac{1}{2}D \sin\theta_2$
$s_2 = r_2 + \frac{1}{2}D \sin\theta_2$.

Echoes from O arriving at Q_2S_2 are correlated with the set of echoes arriving at Q_1S_1, and the displacement estimated for corresponding array elements. Considering just the pair of elements at each end of the arrays, mean displacement and displacement slope give

$\frac{1}{2}((q_2-q_1) + (s_2-s_1)) = r_2-r_1 = \delta r$
$((q_2-q_1) - (s_2-s_1))/D = \sin\theta_2 - \sin\theta_1 = \cos\theta\,\delta\theta$
where $\delta\theta = \theta_2-\theta_1$, $\theta = \frac{1}{2}(\theta_1+\theta_2)$, $\delta r = r_2-r_1$.

Hence ping-to-ping DPCA correlation gives increments in reflector range and look-angle. These are precisely the values needed to preserve phase coherence and focus at the target point along the synthetic aperture. Essentially the same theory holds for a distributed target. The navigation file is corrected by predicting δr and $\delta\theta$ values for each successive pair of pings and then adjusting track and heading to correspond with the correlation values. From Fig 2.1

$r_1 = p_1 + \frac{1}{2}L \sin\theta_1$

$r_2 = p_2 + \frac{1}{2}L \sin\theta_2$

where $\frac{1}{2}L$ is the separation between the DPCA centres and the array centre. For stationary DPCA's, $L \approx$ ping-to-ping platform displacement in the along-track direction. Then

$\delta r = p_2 - p_1 + \frac{1}{2}L(\sin\theta_2 - \sin\theta_1) \approx p_2 - p_1 + \frac{1}{2}L\cos\theta\,\delta\theta$

This shows that the predicted phase-centre displacement δr depends on both θ and $\delta\theta$ for each pair of pings. This holds true whether $\delta\theta$ is determined by autopositioning or derived from the platform heading reference. Errors in $\delta\theta$ and θ, induce range errors, giving phase incoherence in the SAS image. Similar range errors are induced when autopositioning on seabed echoes.

2.2 Beamforming

Echoes received at each DPCA array are formed into overlapping subsets and beamformed towards the selected target area. The equations in 2.1 still apply. Apart from target selection, beamforming has other advantages. Echoes remain well correlated, even when the DPCA's are not stationary in the along-track direction. Correlation displacements are less susceptible to $\frac{1}{2}\lambda$ ambiguities in the presence of noise.

2.3 Simulation Studies

We wished to compare DPCA and centroid heading estimates using similar conditions to the experimental situation described in Section 3. Fig 2.2a shows a simulated SAS image of the T-shaped target used in the experiment, generated using DPCA autopositioning. The target is approximately 1.5m long at a range of about 100 m from the vehicle track. The receiver array was 32 elements long, with λ separation of 15 mm at a centre frequency of 100 kHz. Peak signal/rms noise ratio = 10 dB before pulse compression. Simulated platform speed was 8.5 cm/ping. A sequence of 96 pings was used to form the synthetic aperture. DPCA length was 21 channels, corresponding to a platform movement of 8.25 cm/ping, which is almost the required speed. Each DPCA was then beamformed into 7 overlapping subsets of 15 elements. After autopositioning, rms cross-track error and heading errors were 2mm and 0.8 mr respectively. Experimental processing was complicated by a suspected calibration error between the

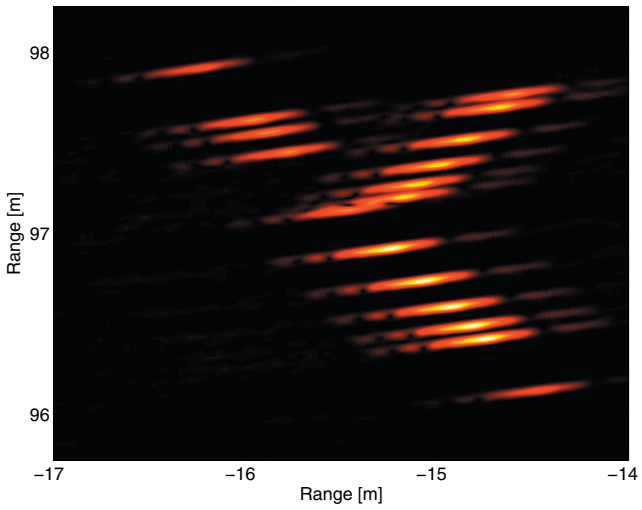

Fig 2.2a. SAS Image of simulated T-target using DPCA autopositioning from true track.

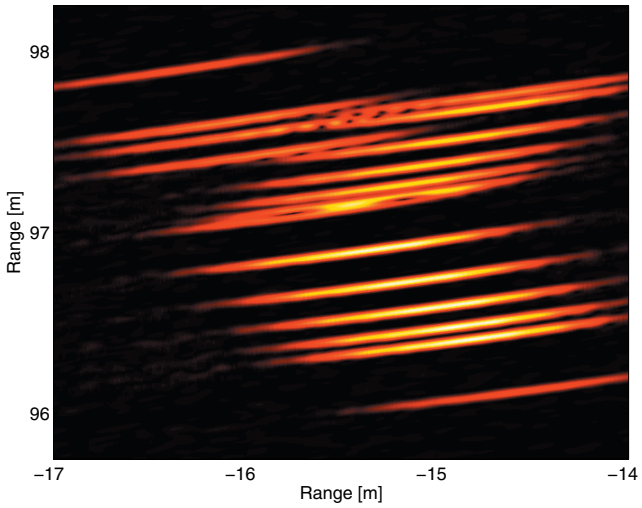

Fig 2.2b. SAS image, using DPCA autopositioning with 0.2 mr calibration error.

leading and trailing DPCA arrays. Figs 2.2b shows the effect of a calibration error of 0.2 mr/ping, accumulating to 19 mr over 96 pings.

2.4. Direct estimation of target look-angle.

DPCA look-angle estimation is inherently incremental. Look-angle to a compact target can be determined directly from the centroid of the physical aperture target image generated at each track position. This location varies due to changing interference patterns between echoes from the target – a problem avoided by the DPCA method - but hopefully this variation averages out if enough reflectors are present. The background of seabed reverberation and noise must be thresholded out before estimating the target centroid.

Heading error was reduced from 0.8 to 0.2 mr sd, corresponding to a centroid azimuth movement of 1.7 cm sd at 100 m range. Centroid variation in range was

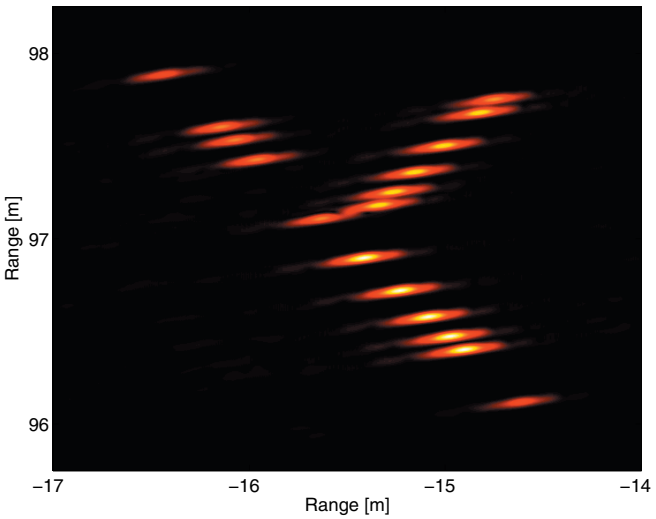

Fig 2.3. Simulated T-Target, autopositioned using centroid look-angle estimation and DPCA range estimation

2.1 cm sd - too large for SAS phase coherence. Hence centroid look-angle estimation was followed by DPCA autopositioning in the range direction. The improved image quality can be seen from Fig 2.3.

The simulated T-target was approximately 1.5m long. Variation of look-angle error with target size was investigated using circular targets containing a random distribution of either 10 or 100 pts/sqm (Fig 2.4).

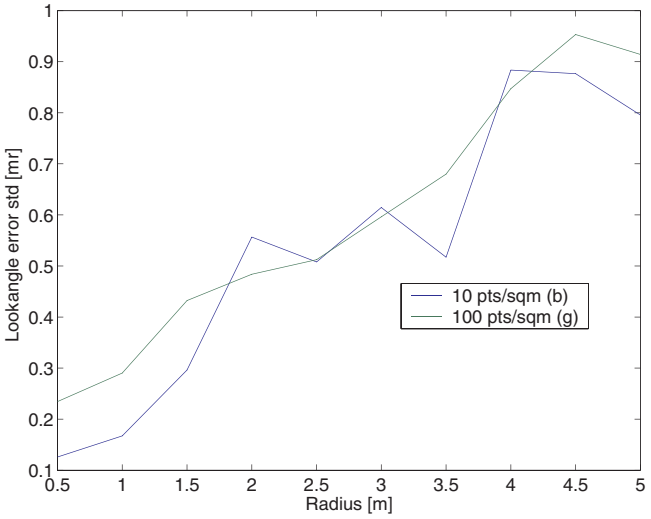

Fig 2.4. Look-angle Error versus Circle Size.

3. ROV Experiment

Two "Mine-Like Object" targets were used, plus the T-target made up from small styrofoam spheres [3] with a target strength of about –35dB. When DPCA autopositioning was used on the T-target for both range and heading, the result is shown in Fig 3.1a. The result using centroid estimation for look-angle followed by DPCA range estimation is shown in Fig 3.1b.

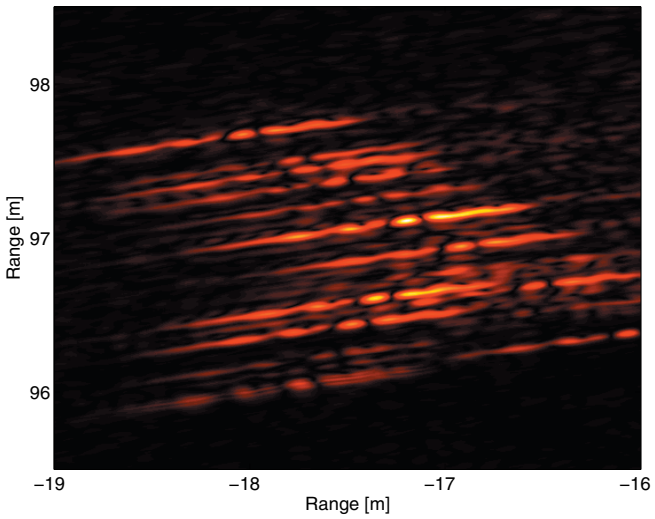

Fig 3.1a. Experimental T-Target using DPCA estimation of look-angle and range.

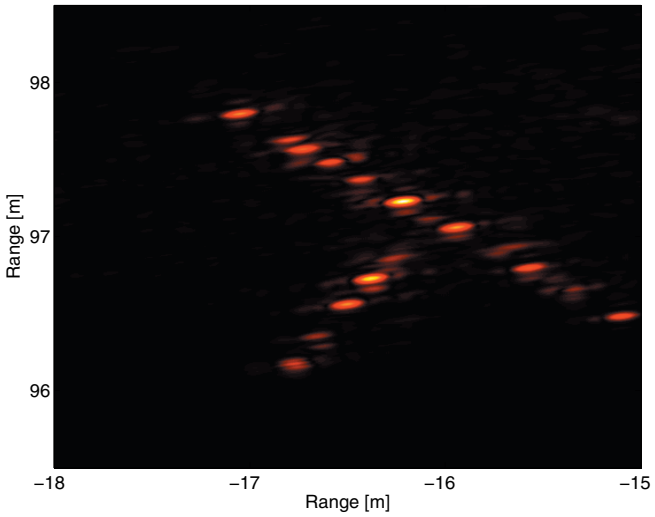

Fig 3.1b. Experimental T-target using centroid look-angle estimation and DPCA range estimation

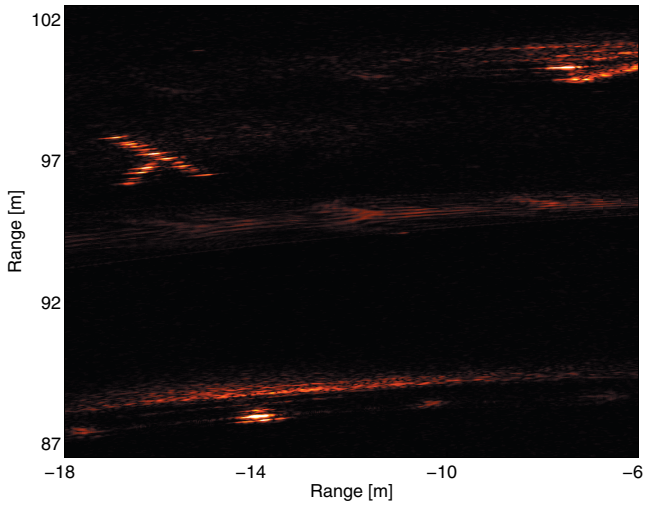

Fig 3.2. Target area using centroid look-angle estimation followed by DPCA track estimation.

Fig 3.2 shows the target area with all three targets. These images were obtaining starting from an assumed straight track with no knowledge of platform speed, heading, depth or attitude variation.

Independent centroid look-angle estimates were available from the three targets. The derived heading angles are compared in Fig 3.3, showing a standard deviation between them of 1mr. The DPCA heading estimate for the T-Target deviates from the mean centroid estimate by 4.7 mr sd.

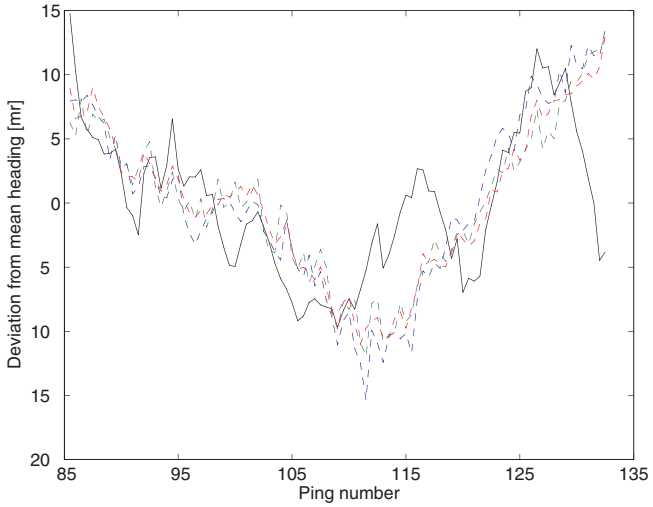

Fig 3.3. Alternative centroid heading estimates (dashed), DPCA heading estimate (solid line).

Heading along the track was estimated using an assumed platform speed. When several targets are available, it is possible to deduce heading errors with no assumption about the track, by registering successive sonar images of the set of targets. Differentiate the rms error between the set of centroids wrt track and heading errors, and then eliminate track errors. In this experiment, the separation between targets was only 10 m, compared with 100 m between targets and platform. The baseline for the heading calculation is target separation, which is here much less than separation between platform and targets. Hence errors increase by an unacceptable factor. However the method could be interesting with wide-angle insonification.

4. Discussion

4.1 Alternative approaches

There is considerable research on estimating mean DOA of signals from a distributed source, mainly originating from mobile telephony, Here, many snapshots seem to be required to achieve reasonable accuracy [4]. However the propagation and correlation problems with wideband sonar are different, so fresh analysis is needed. Image registration using multiple targets or geological structures may also be compared with the image registration problem in medical ultrasonics, also with a large literature, eg [5], though our problem is easier because image deformation should be small or negligible.

4.2 Conclusions

We draw the conclusion from our research that DPCA autopositioning increases image degradation due to heading error. Both in simulation studies and experimental processing, errors were reduced by estimating look-angle directly from the centroid of the physical aperture target image generated from each ping along the track. Small calibration errors lead to unacceptable errors when using the DPCA algorithm to estimate heading. Direct estimation of look angles to 2 m size targets at 100 m range proved more accurate, and enabled good SAS images to be generated with minimal navigation information. Further research is needed both to improve the direct method, and assess where it is superior to DPCA heading estimation, or a commercially available heading reference. However the results given in the paper stengthen the advantages of autopositioning on target rather than seabed echoes, wherever SAS is employed for target identification.

References

[1] A.Bellettini and M.A.Pinto, “Theoretical accuracy of synthetic-aperture sonar micronavigation using a displaced phase-centre array” IEEE J.Oceanic Eng. 27 no.4, pp.780-789, 2002

[2] D.Billon and F.Fohanno, “Two improved ping-to-ping cross-correlation methods for synthetic aperture sonar: theory and sea results”, in Proc OCEANS MTS/IEEE, Biloxi, USA, 29-31 Oct 2002, pp 2284-2293

[3] J.Pihl, P.Ulriksen, O.Kröling, B.Lövgren and G.A.Shippey, “MLO classification using an ROV-mounted wideband synthetic-aperture sonar” in Proc. 5’th E.Conf.on Underwater Acoustics, Lyon, France, 10-13 July 2000, pp 433-438

[4] J. Bach Andersen and K. I. Pedersen, “Angle-of-arrival statistics for low resolution antennas” IEEE Trans. on Antennas and Propagation 50 no.3, pp 391-395, 2002.

[5] F.J.P. Richard and L.D.Cohen, “A new image registration technique with free boundary constraints: application to mammography”, Computer Vision and Image Understanding, 8, pp.166-196, 2003.